REPORT DOCUMENTATION PAGE

1. REPORT DATE (DD-MM-YYYY)	2. REPORT TYPE	3. DATES COVERED (From - To)
	Technical Papers	

4. TITLE AND SUBTITLE

5a. CONTRACT NUMBER

5b. GRANT NUMBER

5c. PROGRAM ELEMENT NUMBER

6. AUTHOR(S)

5d. PROJECT NUMBER
3058

5e. TASK NUMBER
RF9A

5f. WORK UNIT NUMBER

7. PERFORMING ORGANIZATION NAME(S) AND ADDRESS(ES)

Air Force Research Laboratory (AFMC)
AFRL/PRS
5 Pollux Drive
Edwards AFB CA 93524-7048

8. PERFORMING ORGANIZATION REPORT

9. SPONSORING / MONITORING AGENCY NAME(S) AND ADDRESS(ES)

Air Force Research Laboratory (AFMC)
AFRL/PRS
5 Pollux Drive
Edwards AFB CA 93524-7048

10. SPONSOR/MONITOR'S ACRONYM(S)

11. SPONSOR/MONITOR'S NUMBER(S)

12. DISTRIBUTION / AVAILABILITY STATEMENT

Approved for public release; distribution unlimited.

13. SUPPLEMENTARY NOTES

14. ABSTRACT

20030127 094

15. SUBJECT TERMS

16. SECURITY CLASSIFICATION OF:			17. LIMITATION OF ABSTRACT	18. NUMBER OF PAGES	19a. NAME OF RESPONSIBLE PERSON
a. REPORT	b. ABSTRACT	c. THIS PAGE	A		Leilani Richardson
Unclassified	Unclassified	Unclassified			19b. TELEPHONE NUMBER (include area code) (661) 275-5015

21 separate items enclosed

MEMORANDUM FOR PR (Contractor/In-House Publication)

FROM: PROI (TI) (STINFO)   05 Jun 2000

SUBJECT: Authorization for Release of Technical Information, Control Number: **AFRL-PR-ED-TP-2000-110**
Ketsdever, A.; Wong, J., Reed, H. (ASU), "A University Microsatellite as a MEMS-Based Propulsion Testbed"

AIAA Joint Propulsion Conference   **(Statement A)**
(Denver, CO, 14-19 Jun 00)   **(Submission Deadline: 14 Jun 00)**

1. This request has been reviewed by the Foreign Disclosure Office for: a.) appropriateness of distribution statement, b.) military/national critical technology, c.) export controls or distribution restrictions, d.) appropriateness for release to a foreign nation, and e.) technical sensitivity and/or economic sensitivity.
Comments:_____
_____
_____
_____

Signature _____   Date _____

2. This request has been reviewed by the Public Affairs Office for: a.) appropriateness for public release and/or b) possible higher headquarters review.
Comments: _____
_____
_____
_____

Signature _____   Date _____

3. This request has been reviewed by the STINFO for: a.) changes if approved as amended, b.) appropriateness of distribution statement, c.) military/national critical technology, d.) economic sensitivity, e.) parallel review completed if required, and f.) format and completion of meeting clearance form if required
Comments:_____
_____
_____

Signature _____   Date _____

4. This request has been reviewed by PR for: a.) technical accuracy, b.) appropriateness for audience, c.) appropriateness of distribution statement, d.) technical sensitivity and economic sensitivity, e.) military/ national critical technology, and f.) data rights and patentability
Comments:_____
_____

APPROVED/APPROVED AS AMENDED/DISAPPROVED

_____
ROBERT C. CORLEY   (Date)
Senior Scientist (Propulsion)
Propulsion Directorate

AIAA-2000-3670

A UNIVERSITY MICROSATELLITE AS A MEMS-BASED PROPULSION TESTBED

Andrew D. Ketsdever

Air Force Research Laboratory
Propulsion Directorate
Edwards AFB, CA 93524

Joyce Wong and Helen Reed

Arizona State University
Mechanical and Aerospace Engineering
Tempe, AZ 85287

36th AIAA/ASME/SAE/ASEE Joint Propulsion
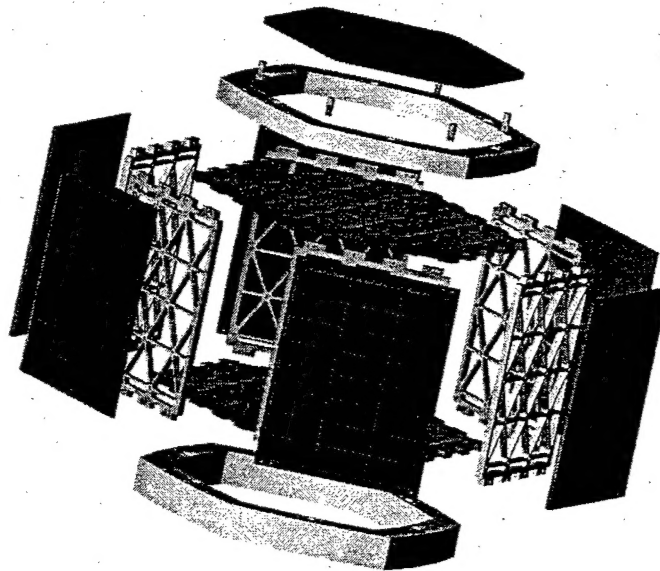Conference and Exhibit
16-19 July 2000
Huntsville, Alabama

A UNIVERSITY MICROSATELLITE AS A MEMS-BASED PROPULSION TESTBED

Andrew D. Ketsdever[1]
Air Force Research Laboratory
Propulsion Directorate
Edwards AFB, CA 93524

Joyce Wong[2] and Helen Reed[3]
Arizona State University
Mechanical and Aerospace Engineering
Tempe, AZ 85287

ABSTRACT

Using reconfigurable and adaptable networks of micro/nanosatellites to support cost-effective space missions is a popular new direction in the space community. Micropropulsion systems, which control a satellite's dynamics and attitude, are instrumental to the success of such missions. Since the overall resources available for a micro/nanosatellite are more restricted than for a single large satellite, the micropropulsion system must be lightweight, low power and low cost. This study provides an initial estimate of the mission requirements that drive a micropropulsion design for a university-built microsatellite. It is demonstrated, through a pragmatic joint venture between a university and a government laboratory, that university satellites are an effective testbed for unconventional new technologies. An example of a university satellite that successfully served as a technology demonstration platform as well as an effective education instrument is presented. A follow-on mission, which will be the platform for flight testing a micropropulsion module, is then described. Two candidate micropropulsion systems, the free molecule micro-resistojet and a cold-gas micronozzle, have been studied for applicability to the prescribed mission. The preliminary study concludes that the free molecule micro-resistojet is the more appropriate micropropulsion system for this particular mission.

[1] Senior Research Engineer, Advanced Concepts Division, Senior Member. andrew.ketsdever@ple.af.mil
[2] NSF Graduate Fellow, Member.
[3] Professor, Director ASUSat, Associate Fellow.

INTRODUCTION

Studies have shown that by partitioning the functions of a single large satellite into a number of smaller satellites that orbit in close proximity and operate cooperatively, one could achieve cost and weight reductions.[1] Such ideas involve a cluster of several to many satellites that fly in formations from 10 to 1000 meters in size. The satellites are in constant communication with each other. Each could perform a unique dedicated task, or the cluster could operate like a parallel computer with each identical satellite contributing a small part to the whole. Hence, the cluster operates cooperatively to perform a function like a "virtual" satellite. These ideas have been applied to the TechSat21 radar mission, and preliminary estimates have indicated that there is merit to this approach.[1] In fact, the New World Vistas Space Technology Panel has advocated the use of networks and clusters of reconfigurable and adaptable micro/nanosatellites to support cost-effective space missions.

A key element for microspacecraft operations is a practical micropropulsion system. Micropropulsion systems offer a wide variety of mission options, all relevant to formation flying, which include attitude control, station maintenance (especially in low Earth orbit (LEO), altitude raising, plane changes, and de-orbit. Consider altitude raising for example. Although the Hohmann transfer is the most efficient means for changing orbit, it requires substantial impulse instantaneously. This can translate into significant power requirements, propellant mass, and a more robust and massive structure. On the other hand, a near-circular spiral transfer, which requires a low-thrust constant burn, may pose less stringent

requirements on the spacecraft. This orbit-transfer scheme is a more attractive alternative for micro/nanosatellites, where the power, volume and mass are not only limited, but might not be scaled proportionally from larger spacecraft. As another example, consider de-orbiting. As individual satellites become useless, there is a strong interest in removing them from LEO to eliminate the growing problem of space debris. For this particular operation that takes place at the end-of-life (EOL) of a satellite, less stringent requirements for the micropropulsion system may be needed. For instance, power usage is generally not critical, pressure regulation may not be required, and lifetime testing can be unnecessary. Consequently, conventional propulsion systems might not be the optimal solution for micro/nanosatellite missions.

The field of micropropulsion is still in its infancy, and further development of current concepts is very much needed. Nevertheless, there are a wide range of new concepts presently being investigated within government agencies, industry, and universities.[1,2] On the whole, the following issues that are generally associated with propulsion systems, would require special attention when dealing with a "scaled-down" system on a micro/nanosatellite:[3]

- Materials compatibility between the propellant and surface material
Even though the compatibility issue between the propellant and surface materials may not exist on larger spacecraft, it can be a problem on micro/nanosatellites due to the materials used in microfabrication processes.

- Contamination problems from propellant ablation and vaporization
This can be attributed to the close proximity of individual micro/nanosatellites in constellation formation.

- Valve leakage
As the propulsion system is scaled down to a micro-level, valve leakage must also decrease proportionally. The operation of micro-valves is dominated by micro-scale transport phenomena that are fundamentally different from those in macro-scale applications.

- Passage clogging that results in single-point failures in micro-machined devices
Micropropulsion systems can be more susceptible to passage clogging because of the micro-scales involved. Innovative approaches to filtering and nozzle design are necessary to ensure functionality and reliability.

- System reliability and durability
As conventional propulsion systems are scaled to a micro-level, every microspacecraft part must perform under the same physical environment as larger spacecraft. The size of the part cannot compromise system reliability and durability. For example, the amount of propellant required by a micropropulsion system may be significantly less than that for a larger spacecraft; however, requirements for the containment of any hazardous propellant remain the same. Moreover, as the physical system is scaled, the mechanical integrity of the system must be preserved.

- Manufacturing complexity
The scale of the product and the selection of materials would require different manufacturing methods. The feasibility and ease of manufacturing—the level of micro-machining technology—can greatly affect the development of micropropulsion systems.

- Integration complexity
There are several components; however, two of the main issues are considered here. First, the internal volume of a micro/nanosatellite is much smaller than that of a larger spacecraft. Consequently, integration of the micropropulsion system with the entire spacecraft must be as simple as possible--involving very few steps, minimal removal of other components, and possibly a modular design to increase flexibility. Second, if part of the micropropulsion system fails after integration, in-situ replacement of the part may be so difficult that replacement of the entire micropropulsion module is preferable. This solution affects the number of backup systems required for a mission.

In order to be useful in micro/nanosatellite operations, micropropulsion systems must be designed to overcome these challenges, while aiming to keep the unit lightweight, compact, low power, efficient, and inexpensive. As can be imagined, overall system considerations enter the selection of a micropropulsion system in addition to performance specific impulse, (I_{sp}) of the propellant.[4] The resources of mass, volume, and power available on micro/nanosatellites will be much more limited than on larger satellites. Hence, additional research, analysis, and testing must be carried out to ensure functionality and mission success.

University Satellites as Technology Testbed

The development of micro/nanosatellite technologies, including micropropulsion, can be achieved through a partnership between government and universities. A university satellite program with its industry and government partners can provide an inexpensive testbed and innovative solutions to satellite technologies. At the same time, such a program is essentially educating and preparing the next generation of scientists and engineers.[4] Another feature of such a program that strongly impacts the students' education is interaction with industry and government. This day-to-day contact brings the students closer to the industry environment and helps students establish a long-lasting network and identify future job opportunities. With the large amount of industry interaction associated with such a project, students also gain confidence in their abilities and develop effective public-speaking and human-interaction skills. Students acquiring these skills at the university level become even more valuable to their profession.

An example of such a program is the Arizona State University (ASU) Student Satellite Program. The design of ASU's first satellite, ASUSat1, began in October 1993, when a local launch vehicle company agreed to launch a small payload for the students if the satellite would perform meaningful science, weigh under 8 kg (including the release mechanism), and fit within an envelope of 33 cm in diameter and 27 cm in height. Due to the size, power, mass and funding constraints, such things as active control, radiation shielding, and many other complex systems were eliminated from the design. Students went through a series of invaluable lessons in search of feasible solutions. These lessons ranged from problem definition, exploring design space, conducting trade studies, determining the feasibility of manufacturing, and quality control. It should be emphasized that these lessons are not taught in the classroom, but were learned hands-on by participating in a real design project. In retrospect, the core objective of the project has been to explore the frontier of the "smaller, faster, cheaper" product space, which is the fundamental challenge to all micro/nanosatellites and all the subsystems that support the mission.

ASUSat1 was one of the lightest satellites designed to do valuable science in space. The science payload included low-cost coarse-resolution spectral imaging, global positioning system (GPS), innovative passive stabilization and damping, 10-degree attitude determination system, autonomous operations, and provision of an audio transponder for amateur radio (AMSAT) operators. The satellite's 14-sided cylindrical body was constructed of a lightweight carbon-fiber composite. There were 510 2 x 2 cm gallium-arsenide (GaAs) solar cells that provided 8 W of power on average for the satellite. The rest of the power system consisted of 6 Nickel-Cadmium batteries and high efficiency DC-DC converters that supplied regulated 3 V and 5 V to the spacecraft subsystems. Other components included dynamics and thermal sensors, a spherical fluid damper, a torque coil, and a gravity-gradient boom.[5,6,7,8]

The collective effort of over 400 students in the 6 years finally came to fruition on January 26, 2000, when ASUSat1 was launched on the maiden voyage of the Orbital/Sub-Orbital Program (OSP) Space Launch Vehicle. Approximately 50 minutes after launch, ASUSat1 was the first of the five payloads to be heard when an amateur radio operator in South Africa received two beacons on its frequency. The contact confirmed that ASUSat1 had been successfully deployed from the rocket and that the satellite was functioning on orbit. Multiple contacts with ASUSat1 were made by amateur radio ground stations around the world. Initial telemetry received from these stations indicated that the satellite was healthy and functioning as expected, except for a possible charging problem. Unfortunately, this problem prevented the solar arrays from supplying power, and the operation of the satellite finally drained the batteries after fifteen hours.

Our mission objective was to show capability in a very low-mass, low-power, low-volume, and low-cost satellite. Even though the mission was brief, telemetry from ASUSat1 indicated that the majority of the student-designed satellite components operated as designed, including the receivers, transmitter, modem, computer, boot-loader software, data acquisition, carbon-composite structure, satellite deployment system, power storage and regulation, boom deployer, gravity-gradient stabilization, and thermal sensors. The signals to ground stations around the world were strong. Attitude sensor data was also obtained, but with only two frames available it is not possible to draw any firm conclusions. Commissioning and analyses of the cameras, GPS, amateur radio repeater, and gravity-gradient fluid damper were scheduled for later in the mission, so no information on these components was available. The ASUSat1 experience was an incredibly positive one for the students. With the wealth of lessons learned from their first satellite, the students are only more eager and ambitious to complete their next mission, the Three Corner Sat (3CS) constellation.

THREE CORNER SAT MISSION

Our next project is a joint effort among ASU, the University of Colorado at Boulder, and New Mexico State University, and thus, aptly named Three Corner Sat.[9] This constellation of three identical satellites shown in Fig. 1 is expected to be inserted by the Shuttle at an initial altitude of 350 km. The spacecraft bus itself is a modular, easily configurable design that allows one to fly multiple science payloads with minimal modifications to the structure and configuration. Also, this program will emphasize student education as students participate in design, manufacturing, integration, testing, mission operations, and program management.

Mission Description

The primary missions of 3CS include stereoscopic imaging, virtual formation flying, innovative communications, automated operations, and end-to-end command and data handling. The stereoscopic imaging mission will take pictures of dynamic atmospheric phenomena using the satellite formation created at deployment. The constellation will make use of creative crosslink communications to aid in distributed and automated operation. This allows both the individual satellites and the formation to reconfigure for optimum data gathering, communications, and command and control.[10,11]

After deployment from the Shuttle, a micropropulsion system will be used to increase the altitude of the satellites, allowing an extended mission lifetime and greater data-gathering capacity. The primary mission requirements are given in the following section.

Spacecraft Description

The individual 3CS satellites will be hexagonal shaped, 45.7 cm across from point to point, and 25.4 cm in height. The primary load-bearing structure is an aluminum 6061-T6 isogrid frame as shown in Figure 2. The panels and the bulkheads are interlocked (Figure 3) in order to provide greater rigidity and flexibility in handling and testing. The top and all side panels will be covered with GaAs solar cells mounted on kevlar and phenelic impregnated aramid honeycomb composite faceplates. The components that will be mounted on the exterior of the top bulkhead are the star mapper, the GPS patch antenna and the top bulkhead solar array. The bottom panel will remain open for sensor access, the micropropulsion module, and the S-band patch antenna as shown in Fig. 4. The top and bottom panels will have a bolt pattern to accommodate either the separation system, or a handling assembly. In addition to the imaging and micropropulsion experiments, other subsystems include the attitude and orbit determination and control subsystem, the communications subsystem, the end to end data subsystem, the electrical and power subsystem, and the structures, mechanisms, thermal, and radiation subsystem.

Current designs have the payload configured as in Fig. 5, so that the transceivers, flight computer, and electrical boxes will be attached to the top bulkhead and side panels. The imager, momentum-wheel assembly, propellant tank, and battery box will be placed on the inside of the bottom bulkhead and will have the capability of attaching to the side panels as well. The payloads in Fig. 5 are general envelopes, as the housings are yet to be designed. Although the propellant tank is modeled as spherical in the envelope drawing, the final shape is to be determined as well.

The 3CS stack will be composed of the three individual spacecraft with separation systems between them. The interface between the satellite stack and Shuttle is the multiple satellite deployment system (MSDS). The basic configuration is shown in Fig. 6. The stack itself will weigh less than 50 kg and will stand 91 cm tall.

Operational Modes

The 3CS mission features eight operational modes. Following separation from the MSDS, the antenna on the bottom spacecraft will be deployed, communication with ground stations will be established, and the stack will go through a functional checkout mode. This mode will last approximately one week. The second mission mode is individual spacecraft separation. Once the correct orientation and pointing of the stack are verified, separation of the individual spacecraft will be initiated by ground command. Upon separation, antennas will deploy from each spacecraft, and communication will be established with ground stations at each university. Telemetry data will be relayed to the ground and health of the spacecraft will be determined accordingly. This phase will last less than one day. The third mode is individual spacecraft functional checkout. Completion of this mode will take approximately one week.

Following spacecraft functional checkout, there will be a performance evaluation mode for both the individual spacecraft and the entire 3CS formation. This mode will assess the formation flying and

virtual communications capabilities. Intersatellite communication links will be used to transfer formation tasks that will best optimize performance. In addition, any shortcomings in individual spacecraft performance will be identified and compensated. This mode will take about two weeks.

The next mode will be the micropropulsion mode in which the micropropulsion system becomes the primary experiment onboard the satellite. It will be used to raise the altitude of the satellites in order to prolong the on-orbit lifetime. The details of this mode will be discussed in the following section.

Once the spacecraft is at an appropriate altitude, the main science operations mode will begin. This mode includes the primary 3CS mission of stereoscopic imaging. Furthermore, throughout this phase the virtual formation network will also be utilized. This primary mission will take approximately eight weeks, but will continue as long as the spacecrafts are operational.

Finally, the micropropulsion experiment will become active again at the end of the proposed science mission. This additional micropropulsion mode will allow the developed thruster system to be fully tested and characterized during the thruster's maiden flight. The additional propellant required for propulsive maneuvers during this experimental mode will be kept within the mass requirements detailed in the following section.

In case of onboard emergency (e.g., the battery voltage falls below a critical value), the flight computer of the affected spacecraft will go into a safe mode. The spacecraft will orient itself into a maximum solar illumination position and transmit and listen at a preprogrammed rate until communication with the ground station is re-established.

Mission Requirements

The objective of the micropropulsion experiment is to demonstrate the functionality of the system by prolonging the in-orbit life of the satellites. After Shuttle deployment, the satellite altitude should be at or above 350 km. If there is no attempt to offset the atmospheric drag, the satellite orbital life is expected to fall short of the requirements imposed by the science mission. As stated earlier, all of the operational modes, with the exception of the micropropulsion mode, require a minimum orbital lifetime of 85 days. This is the strictest requirement for the success of the primary mission. In the case of

shorter orbital lifetimes, some of the scientific results will be compromised. Hence, a possible course of action is either to offset the drag continuously in order to maintain altitude, or to raise orbit to a higher altitude. The trade-off among these options will be discussed in further detail later.

It should be stressed that the satellite mass and power budgets affect the micropropulsion experiment immensely. For instance, the average power produced by the solar array varies between 10 W, using high-efficiency silicon cells, and 15 W with high-efficiency GaAs cells. Housekeeping electronics would require between 3 and 5 W of power, and an active attitude control system would need about 4 W of power. Obviously, not all components can be switched on at the same time. The micropropulsion experiment, consequently, would need to operate on a duty cycle like other electronic components onboard. Also, the internal volume and the mass of the satellite would limit the amount of propellant that can be accommodated and even affect the choice of propellant. Therefore, the method of demonstrating the micropropulsion system must be a compromise between the lifetime of the satellite and the resources available. Current estimates indicate that approximately 10 W of power and 4 kg of mass will be available for the micropropulsion system on the 3CS spacecraft.

Drag Estimates

In order to realistically estimate the drag force on the microsatellite, an accurate prediction of the neutral atmospheric density must be obtained. The most commonly used analytical model of the upper atmosphere is the Mass Spectrometer and Incoherent Scatter (MSIS) model.[12] The MSIS E90 model (1990 version) uses the $F_{10.7}$ flux and a_p geomagnetic index as input parameters. The $F_{10.7}$ flux is a measured quantity of the solar radio flux observed at a wavelength of 10.7 cm. Variations in the 10.7 cm wavelength are used by the model to estimate the long-term variations in solar activity that drives LEO density. Figure 7 shows the measured $F_{10.7}$ from 1991 to January 2000 and the predicted flux (with high and low estimates) through the anticipated 3CS mission timeframe. The predicted values shown in Fig. 7 are used throughout the remaining calculations for the prediction of the drag force anticipated on the 3CS microsatellite.

Figure 8 shows the atmospheric total mass density as a function of orbital altitude for various values of the $F_{10.7}$ flux derived from the MSIS model, and Fig. 8(b) shows the MSIS results for the predicted, low and

high values of the $F_{10.7}$ flux during the launch timeframe. The number density of the major atmospheric components as a function of altitude for a launch predicted value of $F_{10.7} = 139.5$ sfu (1 sfu = 10^{-22} W m^{-2} Hz^{-1}) is shown in Fig. 9. Figure 10 shows the total atmospheric number density throughout the anticipated initial orbit of the 3CS microsatellite assuming a Shuttle deployment. This density is used to estimate the initial drag force that the microsatellite will encounter.

A critical design requirement is that the thrust produced by the micropropulsion system must exceed the atmospheric drag imposed by the neutral atmosphere at the lowest deployable altitude (assumed to be 350 km from a Shuttle launch). In order to calculate the drag force on a spacecraft and subsequently the propellant requirement to overcome the drag, several spacecraft-dependent parameters are required. The ballistic coefficient is defined as

$$B = \frac{m}{C_D A} \qquad (1)$$

where m is the total spacecraft mass, C_D is the coefficient of drag, and A is the total frontal area of the spacecraft (i.e. in the direction of the velocity vector). The drag coefficient ranges from 2 to 4 depending on the gas/surface-interaction processes assumed.[13] A typical value of the drag coefficient for most spacecraft is approximately 2.2.[14] Table 1 shows the anticipated values of the ballistic coefficient for the 3CS microspacecraft.

Table 1. Spacecraft Parameters for 3CS Mission.

Minimum Total Mass (kg)	15
Minimum Cross Sectional Area (m^2)	0.136
Minimum Drag Coefficient[14]	2.0
Maximum Total Mass (kg)	18
Maximum Cross Sectional Area (m^2)	0.150
Maximum Drag Coefficient[14]	2.7
Minimum Ballistic Coefficient (kg/m^2)	37.0
Maximum Ballistic Coefficient (kg/m^2)	66.2

The force due to drag on a spacecraft is given by

$$F_D = \frac{1}{2} m r v^2 B^{-1} \qquad (2)$$

where ρ is the atmospheric density derived by the MSIS model and v is the spacecraft orbital speed at a given altitude.

The maximum drag force extends from 0.04 to 0.14 mN for the range of ballistic coefficients and predicted atmospheric densities [Fig. 8(b)] at the lowest orbital altitude (350 km). Consequently, the minimum thrust from the micropropulsion system should be approximately 2-4 mN to adequately overcome the expected drag force.

The lifetime of an individual 3CS spacecraft as a function of initial deployment altitude is shown in Fig. 11. Figure 12 shows the orbit perigee altitude as a function of the number of orbits for various initial altitudes. The orbital decay and lifetime plots were generated using an industry-standard software package.[15] As mentioned earlier, the science portion of the 3CS mission requires a lifetime in excess of 85 days. The anticipated initial orbital altitude from a Shuttle launch (350 km) yields an expected lifetime of approximately 51 days based on the maximum ballistic coefficient (best case for lifetime calculations) in Table 1. Therefore, the micropropulsion system is required in order to ensure adequate on-orbit time for mission success.

The effects of drag on the individual 3CS satellites can be counteracted in two ways. First, a micropropulsion system can be used periodically to maintain orbit. Second, a micropropulsion system can be used to raise the spacecraft to a specific altitude that can support the desired mission lifetime. A combination of these two methods can allow the spacecraft to be raised to an intermediate altitude that can then be maintained with reduced propulsive requirements.

Table 2 shows the estimated values of the spacecraft lifetime and propulsive requirements. Under the assumed mission operations, the spacecraft will be at an altitude of about 350 km at deployment. Maintaining the orbit at 350 km for approximately 3 months would require a prohibitive Δv, which translates to a large propellant budget. Therefore, the preferred technique would be to raise the orbit of the microsatellite to one which can support a nominal three to four month mission. For the B=66.2 kg/m^2 case (best case), the optimum orbit raising maneuver would be to raise the orbit to between 375 and 400 km initially. Because there are several unknown quantities at this stage of the 3CS development such as actual solar activity and spacecraft ballistic coefficient, an initial orbit raise to 400 km will be opted for in order to allow for error. Table 2 shows the Δv requirements to raise the initial orbit to various altitudes.

6

Table 2. Lifetime and Δv for 3CS spacecraft as a function of altitude.

Final Altitude (km)	Lifetime (days) for B = 66.2 kg/m²	Δv to raise orbit from 350 km (m/sec)
350	58	0
375	100	14.3
400	174	28.6
425	312	42.9
450	584	57.2

Estimated Mission Propulsive Requirements

To achieve the initial science objectives of the 3CS mission, the micropropulsion system will be required shortly after Shuttle deployment to raise each of the 3CS spacecraft to 400 km. Orbit-raising maneuvers performed with a low-thrust propulsion system will require a constant-thrust spiral transfer, which is subjected to pointing errors of the microspacecraft.[15] The utilization of three-axis stabilization is expected to minimize the microsatellite pointing error to within 5°. This will increase the total propellant budget by 3% for the worst-case pointing configuration throughout the altitude-raising maneuver.

Since the initial and final altitudes of the 3CS microspacecraft are rather low, there are no propulsive requirements for de-orbit. However, once the science mission is complete on the 3CS microsatellite, the micropropulsion experiment will begin again. This experiment will thoroughly test the selected micropropulsion system by performing a series of orbit-lowering and -raising maneuvers. The total propulsive budget is given in Table 3 for all potential maneuvers and compensation for losses. Additional maneuvers are desired to assess the micropropulsion system's ability to perform attitude control and demonstrate formation flying. However, they are expected to require minimal propellant.

Table 3. Total Estimated Mission-Required Δv for 3CS

Δv – Drag Makeup (m/sec) – Orbit Raise	28.6
Δv – De-Orbit (m/sec)	0
Δv – Other Maneuvers (m/sec)	100
Δv – Pointing Errors (m/sec)	3.9
Total Δv Required for Mission (m/sec)	132.5

MICROPROPULSION FOR 3CS

Two micropropulsion systems are under consideration for flight on the ASU microspacecraft as a demonstration of unique technology which can be addressed within the pre-launch time frame. The systems currently being considered are the free molecule micro-resistojet (FMMR), which is described in detail elsewhere[16], and a cold-gas micronozzle thruster, which incorporates a laser-machined, 3-dimensional conical nozzle with a throat diameter of 90 μm. Although these two systems do not produce as high a Δv for a given propellant mass as some electrical propulsion systems (e.g. Hall thrusters), their mass and power requirements are a better match for the 3CS constraints.

System Requirements for Free Molecule Micro-Resistojet (FMMR)

The predicted performance characteristics of the FMMR are shown in Figure 13 for a water propellant and a heated-wall temperature of 600 K. These results were derived from numerical simulations using the Direct Simulation Monte Carlo (DSMC) technique.[13,16] The FMMR will operate most effectively for the 3CS mission by utilizing a water propellant stored as ice on orbit. For typical spacecraft temperatures in LEO (260 K), the vapor pressure of ice is approximately 195 Pa which is an ideal stagnation pressure for the FMMR with a 100 μm slot width. This operating pressure gives a thrust per unit slot length of approximately 10 mN/m (Figure 13), which implies that 40 slots with an individual length of 1 cm are required to produce a 4 mN thrust. Although higher values of thrust can be obtained with higher stagnation pressures, there is a distinct advantage to operating the FMMR at low pressures.[16] The FMMR specific impulse at this stagnation pressure is approximately 70.25 sec. As can be seen in Figure 13, smaller thrust required for attitude control can be obtained by reducing the FMMR stagnation pressure (or propellant storage temperature) without significantly compromising the overall efficiency.

Propellant Mass Requirements

The propellant mass required to perform Δv maneuvers is given by

$$m_p = m_o \left[1 - e^{-\frac{\Delta v}{I_{sp} g_o}} \right] \tag{3}$$

where m_o is the initial dry mass of the spacecraft. For the total required Δv given in Table 3, the propellant mass required for the FMMR is approximately 2.45 kg for a spacecraft dry mass of 14 kg. The volume required to store the water propellant would be approximately 0.0029 m^3, allowing a maximum 20% increase in volume as ice expands. Since the FMMR propellant is stored as a liquid at room temperature, the propellant tank need only be designed to survive the launch environment. The largest propellant volume could be contained in a spherical tank with a diameter of 17.8 cm. For a graphite propellant tank, the tank mass would be about 0.4 kg. The composite results are summarized in Table 4 for a Δv of 132.5 m/sec and a dry spacecraft mass of 14 kg.

Power Requirements

The FMMR uses electrical power to heat the thin-film elements which transfer energy into the propellant gas through surface collisions. For the FMMR geometry and operating conditions described by Ketsdever, et al.[16], approximately 6 to 8 W is required to heat the propellant gas to obtain the expected performance. Since the FMMR operates at very low pressures, the valve-sealing requirements are minimized, and the additional power required for valve operations should be minimized.[17] With the use of MEMS-fabricated isolation and actuating valves, the total power required to operate the FMMR can be maintained under 15 W. Pressure regulation inside the device can be achieved by controlling the propellant storage temperature (propellant vapor pressure) with waste heat from the microspacecraft.

Overall System Structure

The FMMR offers several additional benefits from a systems standpoint. First, the long expansion slots are not prone to catastrophic plugging by contaminants. Second, the propellant-feed-system mass and valving requirements are minimized. Third, the micromachined structure is lightweight and robust in construction. In addition, the entire slot assembly for the FMMR geometry of 40 slots with a width of 100 μm can be contained within a 2.5 cm x 2.5 cm area. Plus the added benefit of launching a benign propellant at atmospheric pressure makes the FMMR very attractive, especially in the case of the proposed Shuttle launch. Lastly, the total FMMR system mass will be approximately 3.3 kg including propellant.

System Requirements for Cold-Gas Micronozzle

The cold-gas (CG) micronozzle thruster has a throat diameter of 87.6 μm, an exit diameter of 257 μm, and a supersonic expansion angle of 15°. To provide a thrust of approximately 10 mN with a molecular nitrogen propellant, the CG thruster will be required to operate at a stagnation pressure of 10^6 Pa. At these conditions, the anticipated specific impulse for this thruster is 80.3 sec.

Propellant Mass Requirements

Following the same analysis developed for the FMMR, the propellant mass required for the CG micronozzle thruster to perform the required mission is 2.17 kg. The minimum design operating pressure for the CG thruster is approximately 10^5 Pa, which indicates that some propellant will remain in the feed system at the spacecraft EOL. Based on the assumption that no propellant will be lost due to valve leakage, this implies that 0.7% more propellant mass will need to be stored in order to perform the mission based on the same Δv requirements. However, valve leakage can be a major concern with high-pressure systems.

The use of gaseous propellant on microspacecraft has two serious drawbacks. First, the relatively low density of the propellant requires large storage volumes on extremely space-limited microspacecraft. Second, gaseous propellants must be stored at high pressures which requires relatively massive fortified propellant tanks when compared to propellant mass. For example, a graphite propellant tank containing nitrogen stored at 20 MPa will require a mass approaching 1.3 kg. To reduce the storage volume, the storage pressure can be increased; however, the tank mass may increase to unacceptable levels.[16] The CG system requirements are summarized in Table 4.

Power Requirements

Unfortunately, the use of a CG micronozzle thruster does not come at reduced power consumption. Since the propellant storage pressure is roughly 200 atmospheres, a valve is required with an extremely low leak rate. Typically these valves require power to open on the order of 10 to 30 W.[18] However, lower power valves with increasingly lower leak rates are currently being developed even on the MEMS level [19]. In this general survey, it is assumed that the power supply mass for the CG thruster is equivalent to that required for the FMMR.

Overall System Structure

The CG micronozzle thruster has several disadvantages from an overall systems viewpoint; however, the technology has been previously

demonstrated. The CG micronozzle system will require high-pressure feed lines, pressure regulation, and strict propellant filtering due to an additional concern of catastrophically plugging the nozzle throat. The total CG propulsion system mass will be approximately 4.5 kg including propellant.

Table 4. Micropropulsion System Comparison

Thruster	FMMR	CG
Propellant	Water	N_2
Thrust (mN)	4-6	5-10
Isp (sec)	70.3	80.3
Propellant Mass (kg)	2.45	2.17
Empty Propellant Tank Mass (kg)	0.4	1.3
Full Propellant Tank Mass (kg)	2.85	3.47
Spherical Tank Radius (cm)	8.9	15.8
Estimated Power Requirement (W)	15	10-20

MICROPROPULSION SYSTEMS ANALYSIS

In an attempt to quantify the fundamental viability of the FMMR, an initial systems comparable or effective specific impulse has been estimated.[3] The effective Isp modifies the thruster's intrinsic Isp by taking into account such system losses as high pressure propellant storage, MEMS valve leakage, and propellant left over in the storage system at the spacecraft end of life (EOL). *already defined on page 2*

For an overall systems analysis of microthruster systems, it is important to consider other sources of mass in addition to the propellant. One of these major sources is the propellant storage tank. For a nitrogen propellant stored at 20 MPa and 300K in a spherical titanium (ultimate tensile strength = 1.23 GPa) tank, the ratio of the tank mass to the propellant mass is approximately 1.0 using a safety factor of 2. Similar analysis for an graphite tank yields a mass ratio of 0.483. For microthruster systems which use propellant stored as high pressure gases, the storage tank mass can be on the same order as the propellant mass required to perform the mission.

sigma = 1.23 (handwritten margin note)

Effective Specific Impulse

The effective specific impulse of a thruster system in terms of the extra mass associated with minimum operating pressure, propellant loss due to valve leakage, and storage tanks can be given by[3]

$$I_{sp.eff} = \frac{I_{sp}\left[1 - \dfrac{p_{o,d}}{p_{i,s}}\right]}{(1+\zeta)\left[1 + \dfrac{M_t}{M_{p,s}}\right]} \qquad (4)$$

where Isp is the intrinsic specific impulse of the thruster, $p_{o,d}$ is the design operating pressure of the thruster, $p_{i,s}$ is the initial propellant storage pressure, ζ is the fraction of propellant lost due to valve leakage, M_t is the propellant tank mass, and $M_{p,s}$ is the mass of the stored propellant.

Effective Specific Impulse Comparisons of the FMMR with a Cold Gas Thruster

As mentioned earlier, the operating characteristics of the FMMR appear very attractive using a water propellant stored on-orbit in solid form. Table 4 lists the intrinsic Isp of the FMMR operating on water propellant with Kn = 1 and T_w = 600K to be approximately 70 sec.

The propellant storage pressure (i.e., the vapor pressure for a solid propellant) being extremely small (on the order of 10^2 Pa maximum) has several advantages from a systems viewpoint. First, the storage tank need only be designed to handle launch stresses since the storage pressure is much less than the ultimate tensile strength of most materials. In this case, standard materials such as titanium, aluminum, and graphite can be replaced by much lighter materials. Second, the reduced storage pressure lowers the leak rate through MEMS valves to trivial levels ($\zeta \approx 0$). Third, since $p_{o,d}$ is unusually small, nearly all of the propellant is used by the FMMR at EOL ($p_{o,d} \approx p_{i,s}$). From these arguments, the effective Isp for the FMMR is very close to its intrinsic value of 70 sec.

Table 5 gives a general comparison between the FMMR operating with a water propellant and micronozzle systems which store high pressure helium, nitrogen and argon propellants as a function of the operating temperature. The effective Isp results for the micronozzle cases are also shown for various values of ζ. In the case of the FMMR, the operating temperature is T_w, and in the case of the micronozzle, the operating temperature is the stagnation temperature. For a cold gas micronozzle thruster (20 μm diameter throat, outlet to throat area ratio of 20, and expansion angle of 15°) operating on a gaseous nitrogen propellant, the ideal intrinsic specific impulse is approximately 80 sec. Assuming that there are no viscous losses in the micronozzle,

Insert Table 5 after → this page (handwritten note)

the minimum design pressure will be 0.1 MPa (Re ≈ 400). A graphite propellant tank is assumed with a storage pressure of 20 MPa. If it is assumed that $\zeta = 0$, the effective Isp for the nitrogen cold gas micronozzle is approximately 54 sec.

The FMMR can operate with a water or ammonia propellant in a cold gas mode (i.e. with the heating elements off) without the problem of the propellant recondensing in the device. This is due to the low operating pressure and short residence time of water on surfaces with a temperature of 300 K. Cold gas micronozzle flows on the other hand will experience some degree of condensation in the stagnation region which acts to seriously degrade performance.

It is evident from Eqn. (4) that the mass of the propulsion system's power supply has not been included in the calculation of effective specific impulse. In this case, it is assumed that the power supplies and related plumbing required for the FMMR and the cold and warm gas micronozzles will be roughly the same. Cold gas thrusters which operate at high pressures typically require heavy, high power valves, thick walled tubing, and pressure regulators which tend to balance out the weight of the FMMR power supply.

Propellant Storage Volume Considerations

Although microspacecraft may be mass and power limited, perhaps the most critical obstacle for the propulsion subsystem is the severe volumetric limitation. Obviously, there is a benefit in storing solid or liquid propellants over gaseous propellants in terms of reduced storage volume. The volume required to store the propellant is a function of the mission requirements (i.e. Δv required) and the density of the propellant. However, the mass of the propellant stored at the beginning of the mission $M_{p,s}$ depends on the minimum operating pressure of the thruster and the valve leak percentage.

If it is assumed that the initial mass of the spacecraft will differ between the high pressure micronozzle operation and the FMMR only in the mass of the propellant storage tank, then in the limit of small Δv the ratio of propellant storage tank volume becomes

$$\frac{V_{t,MN}}{V_{t,FMMR}} = \frac{\rho_{p,FMMR}}{\rho_{p,MN}} \left[\frac{Isp,eff_{FMMR}}{Isp,eff_{MN}} \right] \quad (5)$$

where ρ_p is the density of the propellant, Isp,eff is the effective Isp derived from Eqn. (4), and the terms with subscript MN refer to the micronozzle values.

In the case used previously for a cold gas nitrogen micronozzle expansion with the propellant stored at 20 MPa and $\zeta = 0$, the propellant density (To = 300K) and effective specific impulse are 224.5 kg/m3 and 54.1 sec, respectively as shown in Table 5. For the FMMR operating on water vapor (from propellant stored as ice) with T_w = 600K, the effective specific impulse is 70 sec. Therefore, the ratio from Eqn. (5) is approximately 5.6 for a graphite storage tank. For a titanium propellant tank, the storage volume ratio is approximately 22. Although factors of 2 to 3 reduction in the volume ratio can be envisioned by storing the nitrogen propellant at higher pressure, there are material limitations to this approach.

CONCLUSIONS

The FMMR and cold gas systems are chosen among other micropropulsion technologies because their mass and power requirements fit well with the 3CS mission requirements. Moreover, the simplicity and maturity of the technology also promises a functional system to be completed within the two-year pre-launch timeframe. Although both micropropulsion systems can satisfy similar operational requirements, the FMMR has several beneficial systems characteristics, which makes it the more attractive system for 3CS. For example, the propellant storage volume is greatly reduced over the high-pressure cold gas system, the total system mass is reduced, the geometry of the FMMR is easy to machine and quite robust, and the expansion slots are less susceptible to catastrophic clogging compared to the single point failure of the cold gas nozzle throat.

The mission presented is a worst-case scenario in which 3CS micropropulsion experiment begins at 350 km. With a higher Shuttle insertion of 400 km, the micropropulsion system requirements for mass, volume, and power will be reduced. Moreover, trading on-orbit lifetime for smaller resource usage provides another possibility. A number of system trades will be considered over the next several months of design in order to maximize the potential information derived from the 3CS mission. Based on the current study, the results for flight testing the FMMR are encouraging and suggest the success of the FMMR as a candidate for future microspacecraft propulsion.

ACKNOWLEDGEMENTS

Program, Lockheed Martin Management & Data Systems, Honeywell Space Systems Group, Motorola, AFRL-Edwards AFB, AFRL–Kirtland AFB, SpaceQuest, Intel, and Microchip.

REFERENCES

1. Proceedings of the Workshop on AFRL Formation Flying and Micropropulsion, Lancaster, CA, October 20-21, 1998.

2. Proceedings of the Workshop on AFOSR/DARPA AFRL/VSD Micro/ Nanotechnology for Micro/Nanosatellites, Albuquerque, NM, April 21-22, 1998.

3. Ketsdever, A., Wadsworth, D., and Muntz, E., "Predicted Performance and Systems Analysis of the Free Molecule Micro-Resistojet", submitted to AIAA Progress Series on Micropropulsion, 2000.

4. Ferring, S., Lenz, C., Friedman, A., and Reed, H., "ASUSat Lab - Past, Present, and Future", AIAA paper 99-0802, Reno, NV, January 1999.

5. Friedman, A., Ferring, S., Lenz, C., Reed, H., and Underhill, B., "ASUSat1: The Development of a Low-Cost Satellite", Proceedings of the 16th Space Symposium and AMSAT-NA Annual Meeting, UK, pp. 141-155, The American Radio Relay League, Inc., Newington, CT, July 1998.

6. Rademacher, J., Reed, H., and Puig-Suari, J., "ASUSat 1: An Example of Low-Cost Nanosatellite Development", Acta Astronautica, Volume 39, Number 1-4, Pages 189-196, 1996.

7. Friedman, A., Underhill, B., and Reed, H., "ASUSat1 – On-Orbit Operations and Satellite Profile", Proceedings of the 17th Space Symposium and AMSAT-NA Annual Meeting, San Diego, pp. 55-60, The American Radio Relay League, Inc., Newington, CT, October 8-10, 1999.

8. Underhill, B., Friedman, A., and Reed, H., "Dynamics and Control of Nanosatellite ASUSat1", American Astronautical Society, AAS 00-063, Breckenridge, CO, February 2-6, 2000.

9. Underhill, B., Friedman, A., Wong, J., Reed, H., Hansen, E., Colaprete, T., Rodier, Horan, S., and Anderson, B. "Three Corner Sat Constellation – Arizona State University: Management; Electrical Power System; Structures, Mechanisms, Thermal, and Radiation; Attitude / Orbit Determination and Control; ASU Micropropulsion Experiment; and Integration", SSC99-III-1, 13th Annual AIAA/USU Conference on Small Satellites, Logan, UT, August 23-26, 1999.

10. Hansen, E., Colaprete, T., Rodier, D., Friedman, A., Underhill, B., Wong, J., Reed, H., Horan, S., and Anderson, B. "Three Corner Sat Constellation: C&DH, Stereoscopic Imaging, and End-to-End Data System", SSC99-IV-1, 13th Annual AIAA/USU Conference on Small Satellites, Logan, UT, August 23-26, 1999.

11. Horan, S., Anderson, B., Underhill, B., Friedman, A., Wong, J., Reed, H., Hansen, E., Colaprete, T., and Rodier, D. "Three Corner Sat Constellation – New Mexico State University: Communications, LEO Telecommunications Services, Intersatellite Communications, and Ground Stations and Network", SSC99-VI-7, 13th Annual AIAA/USU Conference on Small Satellites, Logan, UT, August 23-26, 1999.

12. Hedin, A.E., "Extension of the MSIS thermospheric model into the middle and lower atmosphere", Journal of Geophysical Research, Vol. 96, pp. 1159-72, 1991.

13. Bird, G., Molecular Gas Dynamics and the Direct Simulation of Gas Flows, Oxford University Press, New York, 1994.

14. Larson, W., and Wertz, J., Space Mission Analysis and Design, Second Edition, Microcosm-Kluwer, Torrance, CA, 1992.

15. Website: http://www.stk.com, Satellite Tool Kit, Analytical Graphics, Inc., 2000.

16. Ketsdever, A., Wadsworth, D., and Muntz, E., "Performance, Systems, and Design Considerations for a Free Molecule Micro-Resistojet for Nano/Microspacecraft Thrust Generation", Presented at the Nanospace '98 Conference, Houston, TX, November 2-6, 1998.

17. Janson, S., and Helvajian, H., "Batch-Fabricated Microthrusters: Initial Results", AIAA paper 96-2988, July 1996.

18. Bzibziak, R., "Miniature Cold Gas Thrusters", AIAA paper 92-3256, July 1992.

19. Sim, D., Kurabayashi, T., and Esashi, M., "A Bakable Microvalve with a Kovar-Glass-Silicon-Glass Structure", Journal of Micromechanics and Microengineering, Vol. 6, No. 1, 1996, pp. 266-271.

Table 5: Comparison of Effective Specific Impulse for the FMMR and Cold/WarmGas Micronozzle (MN) Cases.

Thruster (Propellant)	T_o (K)	$\dfrac{M_t}{M_{p,s}}$ (Graphite)	ζ	Intrinsic Isp (sec)	Effective Isp (sec)	$\dfrac{V_t}{V_{t,FMMR}}$
FMMR (H_2O)	300	0.0015	0	48.1	48.1	1
FMMR (H_2O)	600	0.0015	0	70.3	70.3	1
MN (He)	300	6.8	0	253.7	32.7	129.8
MN (He)	300	6.8	0.1	253.7	29.7	142.7
MN (He)	300	6.8	0.2	253.7	27.2	155.7
MN (He)	600	6.8	0	358.7	46.2	91.8
MN (He)	600	6.8	0.1	358.7	42.0	100.9
MN (N_2)	300	0.48	0	80.3	54.1	5.6
MN (N_2)	300	0.48	0.1	80.3	49.2	6.2
MN (N_2)	600	0.48	0	113.6	76.6	4.0
MN (Ar)	300	0.34	0	56.7	42.4	5.0
MN (Ar)	300	0.34	0.1	56.7	38.5	5.5

insert Table 5
before page 10's
all other tables are
shown after referenced
in text.
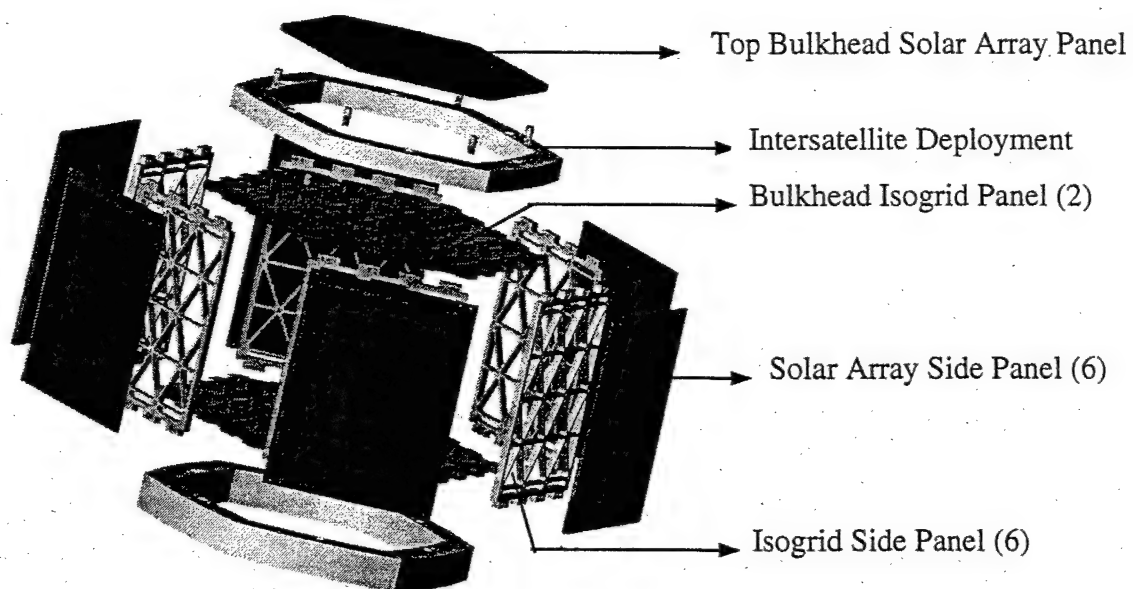
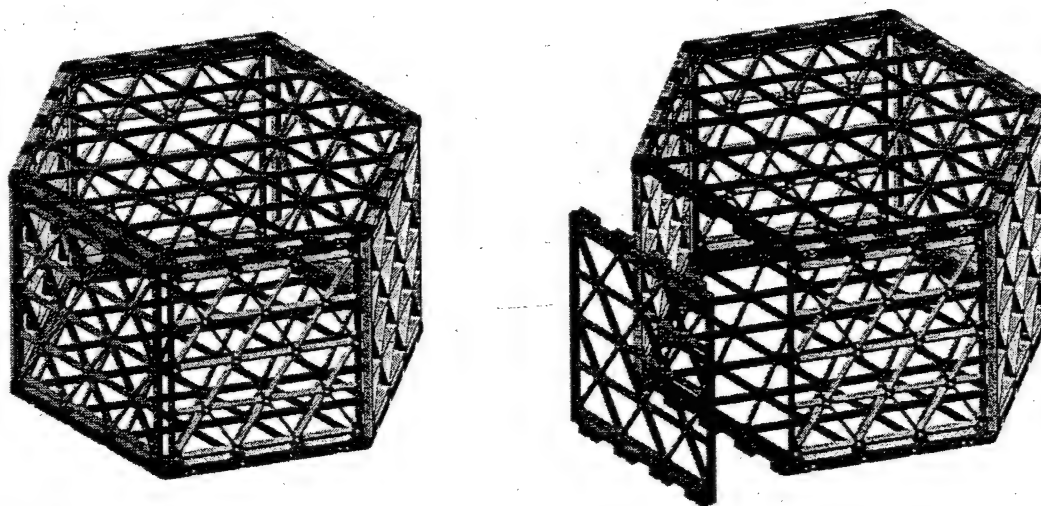Figure 1. Typical structure of an individual 3CS microspacecraft.
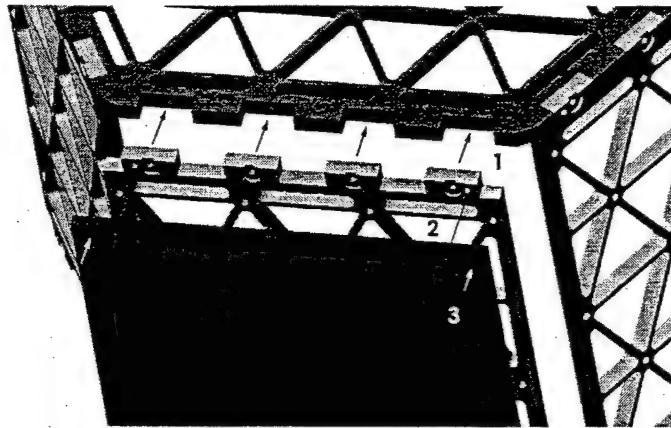

Figure 2. 3CS isogrid structure.

Figure 3. Blow-up view of the satellite structure. The isogrid side panel (2) and the bulkhead (1) are interlocked in order to provide greater rigidity. The composite solar array substrate (3) will be mounted to the side panels in four places with two mounts on the top and two on the bottom.
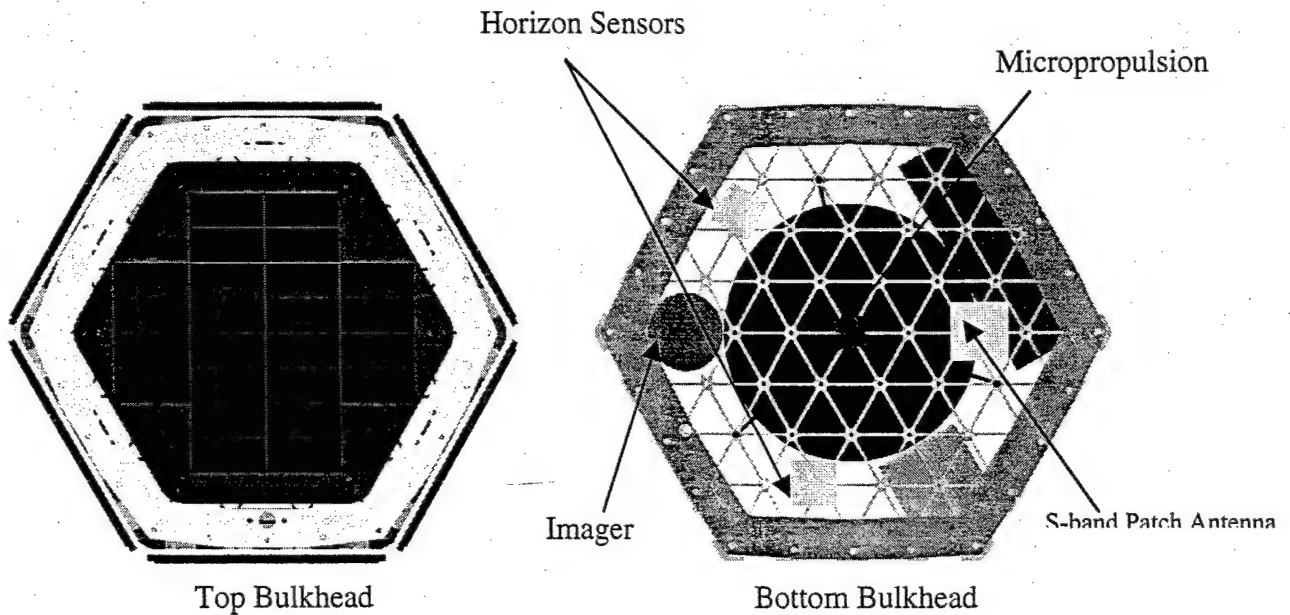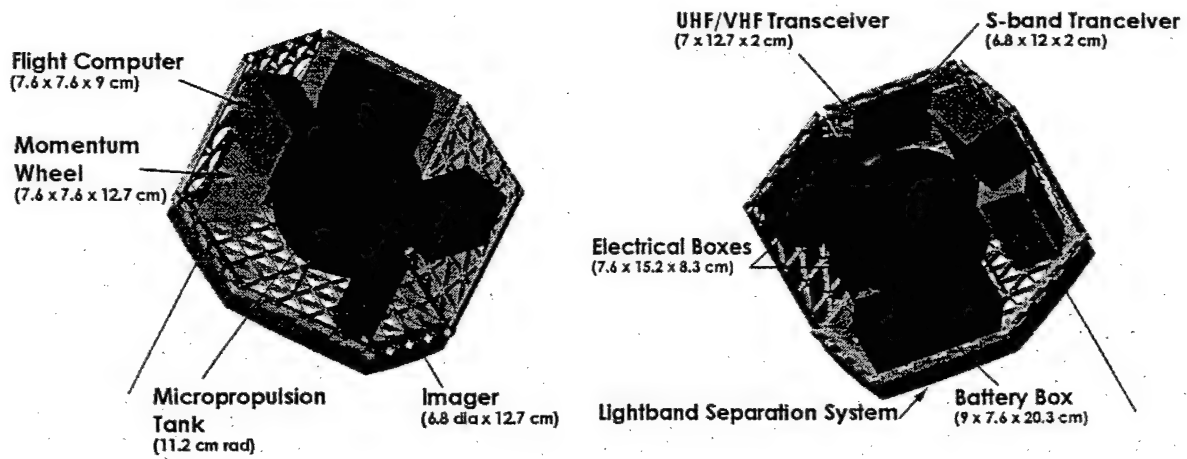

Horizon Sensors

Micropropulsion

Imager

S-band Patch Antenna

Top Bulkhead

Bottom Bulkhead

Figure 4. Microspacecraft bulkheads.

Flight Computer
(7.6 x 7.6 x 9 cm)

Momentum
Wheel
(7.6 x 7.6 x 12.7 cm)

Micropropulsion
Tank
(11.2 cm rad)

Imager
(6.8 dia x 12.7 cm)

UHF/VHF Transceiver
(7 x 12.7 x 2 cm)

S-band Tranceiver
(6.8 x 12 x 2 cm)

Electrical Boxes
(7.6 x 15.2 x 8.3 cm)

Lightband Separation System

Battery Box
(9 x 7.6 x 20.3 cm)

Figure 5. Internal component placement.

Sparky
(S/C 1)

Ralphie
(S/C 2)
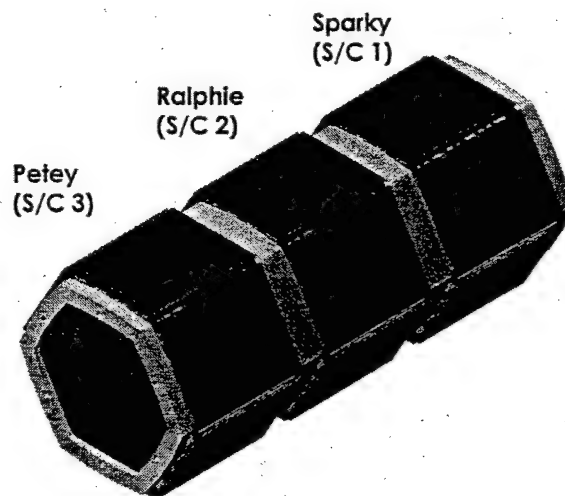
Petey
(S/C 3)

Figure 6. 3CS stack configuration. The satellites are named after the school mascots: Petey (NMSU); Ralphie (CU); and Sparky (ASU).

PAGES _16 fig 7,8_
ARE
MISSING
IN
ORIGINAL
DOCUMENT
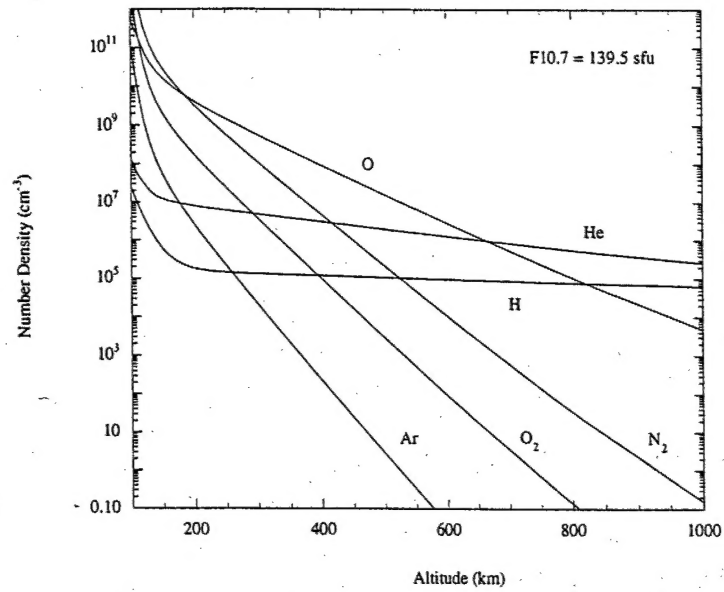
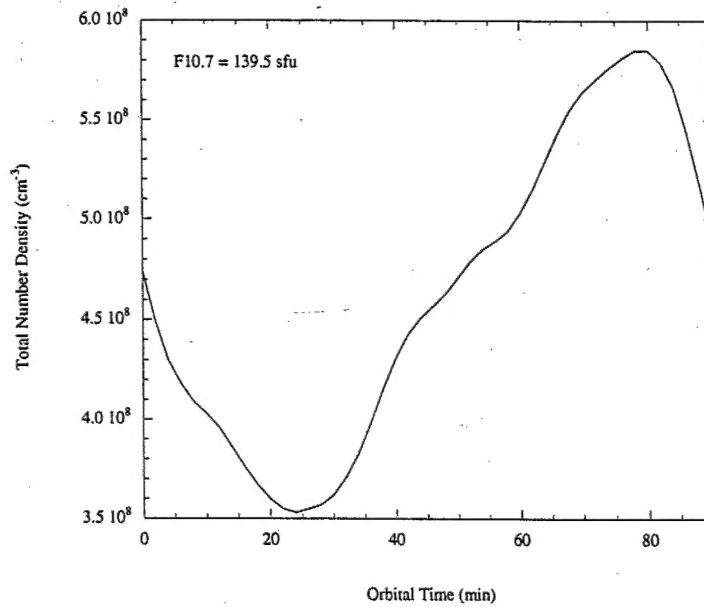Figure 9: Atmospheric number density of various constituents as a function of altitude.

Figure 10: Total atmospheric number density as a function of spacecraft orbit time for an initial orbital altitude of 350 km.
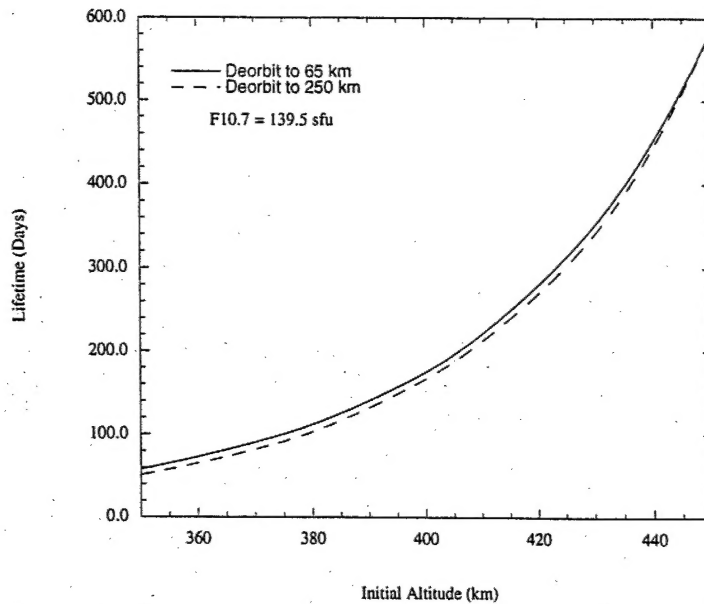
Figure 11: Predicted lifetime versus initial orbital altitude for B = 66.2 kg/m² (F10.7 = 139.5 sfu). Solid line: lifetime for final altitude of 65 km. Dashed line: lifetime for final altitude of 250 km.

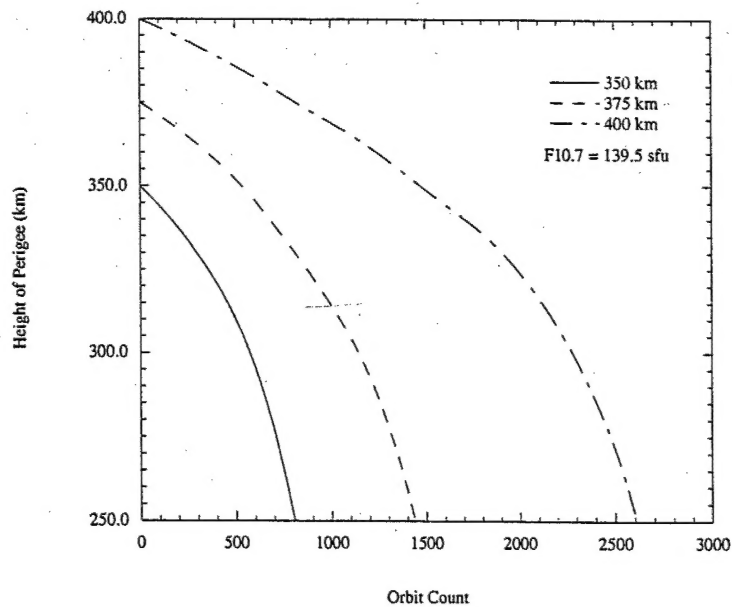Figure 12: Perigee height as a function of orbit number for various initial altitudes (B = 66.2 kg/m², F10.7 = 139.5 sfu).
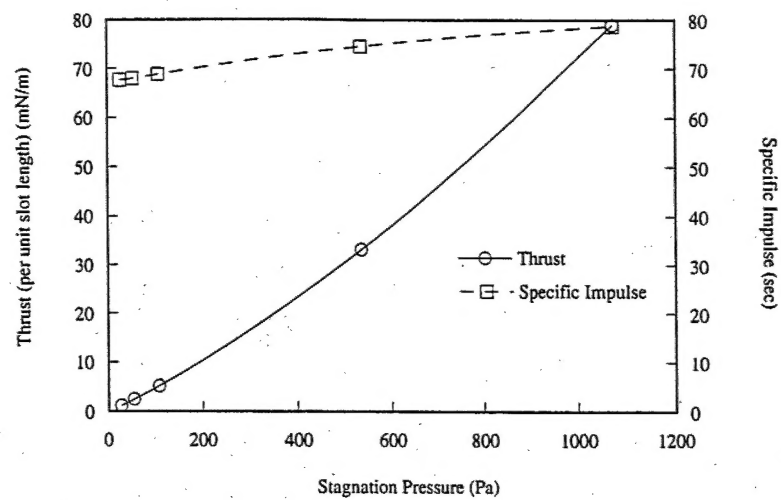
18

Figure 13: Predicted FMMR performance characteristics as a function of operating pressure assuming a heated wall temperature of 600 K and a water propellant.